PREPARED FOR THE U.S. DEPARTMENT OF ENERGY,
UNDER CONTRACT DE-AC02-76CH03073

PPPL-3803
UC-70

PPPL-3803

A New Method for Simultaneous Measurement of the Integrated Reflectivity of Crystals at Multiple Orders of Reflection and Comparison with New Theoretical Calculations

by

S.G. Lee, J.G. Bak, Y.S. Jung, M. Bitter,
K.W. Hill, G. Hoelzer, O. Wehrhan, and E. Foerster

April 2003

PPPL
PRINCETON PLASMA
PHYSICS LABORATORY

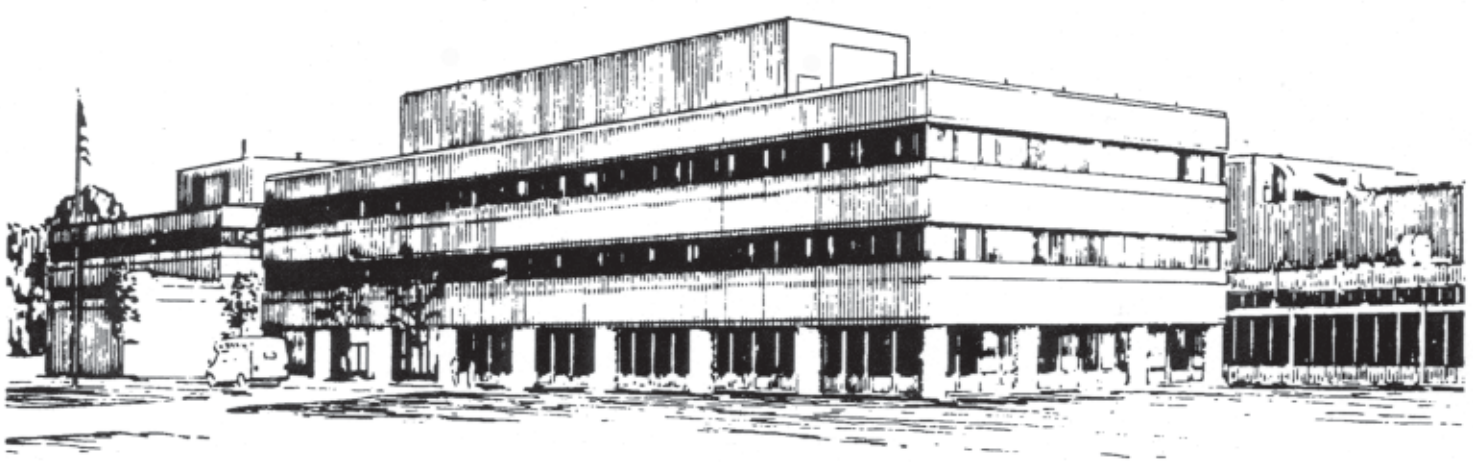

PRINCETON PLASMA PHYSICS LABORATORY
PRINCETON UNIVERSITY, PRINCETON, NEW JERSEY

PPPL Reports Disclaimer

Availability

This report is posted on the U.S. Department of Energy's Princeton Plasma Physics Laboratory Publications and Reports web site in Fiscal Year 2003. The home page for PPPL Reports and Publications is: http://www.pppl.gov/pub_report/

DOE and DOE Contractors can obtain copies of this report from:

U.S. Department of Energy
Office of Scientific and Technical Information
DOE Technical Information Services (DTIS)
P.O. Box 62
Oak Ridge, TN 37831

Telephone: (865) 576-8401

Fax: (865) 576-5728

Email: reports@adonis.osti.gov

This report is available to the general public from:

National Technical Information Service
U.S. Department of Commerce
5285 Port Royal Road
Springfield, VA 22161

Telephone: 1-800-553-6847 or
(703) 605-6000

Fax: (703) 321-8547

Internet: http://www.ntis.gov/ordering.htm

A new method for simultaneous measurement of the integrated reflectivity of crystals at multiple orders of reflection and comparison with new theoretical calculations*

S. G. Lee[a*], J. G. Bak[a], Y. S. Jung[a], M. Bitter[b], K. W. Hill[b],
G. Hoelzer[c], O. Wehrhan[d] and E. Foerster[d]

[a]Korea Basic Science Institute, Yusung, Taejeon 305-333, Korea,

[b]Princeton Plasma Physics Laboratory, Princeton, NJ 08543, U. S. A.,

[c]X-Fab Semiconductor Foundries AG,
Haarbergstrasse 61, 99097 Erfurt, Germany

[d]Friedrich-Schiller University, Jena, Germany,

ABSTRACT

The paper describes a new method for the simultaneous measurement of the integrated reflectivity of a crystal for multiple orders of reflection at a predefined Bragg angle. The technique is demonstrated with a mica crystal for Bragg angles of 43°, 47°, and 50°. The measured integrated reflectivity for Bragg reflections up to the 24th order is compared with new theoretical predictions, which are also presented in this paper.

***Provisional Patent Application No: 60\378,549**

PACS numbers: 61.10-i, 52.25.Nr

---

*e-mail: sglee@kbsi.re.kr

1. INTRODUCTION

In a previous paper[1], Lee et al. described a new method of measuring the integrated reflectivity of a crystal by using the bremsstrahlung continuum from an X-ray tube in combination with an energy resolving X-ray detector. The method offers many advantages over the previously used technique and, due to the fact that it simultaneously determines the integrated reflectivity for all orders of reflection at a predefined Bragg angle, it is especially well suited for calibration of crystal spectrometers, which find wide applications in research and industry.

The measurements described in reference 1 were carried out with a mica crystal at a Bragg angle of 45° for Bragg reflections up to the 22nd order. Mica is distinctly different from most other crystals, since the integrated reflectivity for certain higher order Bragg reflections is larger than that of the lowest order. Because of these unusual properties, mica is ideally suitable for testing the new method as well as for validation of theoretical predictions. Calculations of the integrated reflectivity of mica for multiple orders of reflection at a predefined Bragg angle have recently been published by Hoelzer et al.[2] These calculations are directly applicable to the experimental arrangement used in reference 1 and in this paper.

In reference 1, theoretical predictions[2] of the integrated reflectivity of mica for Bragg angles in the range from 50° to 89° were extrapolated to a Bragg angle of 45°; these extrapolations were found to be in good qualitative agreement with the experimental data. Furthermore, quantitative agreement between the extrapolated values and the experimental data was obtained for a limited range of orders of reflection depending on the order of the Bragg peak used for normalization of the observed integrated reflectivity to the corresponding predicted value. However, with the comparison performed in reference 1, quantitative agreement between experiment and theory could not be produced for the entire

spectrum of Bragg peaks. The *apparent* discrepancies between experiment and theory gave rise to questions about possible systematic errors in the measurement or interpretation of the data. It was also argued that the above-mentioned extrapolation of the theoretical predictions[2] might not be justified, since the Bragg angle of 45° corresponds to an energy near the K-absorption edge of aluminum, which is a constituent of mica.

In order to address these questions, we have performed additional measurements for Bragg angles of 43°, 47° and 50°, which correspond to energies below and above the Al K-absorption edge, and have compared these experimental results with new theoretical calculations for these specific Bragg angles. The code used for these new calculations is described in reference 3. We also repeated the measurement of the bremsstrahlung spectrum from the X-ray tube, taking great care to insure that the experimental arrangement of the detector with respect to the vacuum window was exactly the same as for the measurements of the Bragg peaks. These steps were taken in order to eliminate any experimental errors which might result from differences in absorption in air due a different length of the air gap between window and detector. Moreover, we investigated the effects of weak fluorescent peaks on the measurement of the integrated reflectivity for certain orders of reflection. In the course of these investigations we discovered that the apparent discrepancies found in reference 1 were due to an error in the data analysis. After elimination of this error the experimental data are now in quantitative agreement with Hoelzer's theory for the entire spectrum of Bragg peaks, except for the 12^{th} and 18^{th} order of reflection. Since these new results are important for an experimental verification of the theory and a validation of our method, a detailed description of the experiments - including figures for each of the investigated Bragg angles - and data analysis is given in this paper for future reference.

The paper is organized as follows: The experimental arrangement is described in section 2. The experimental results are presented in section 3. A discussion of the advantages of the new method of measuring the integrated reflectivity is in section 4. Conclusions are presented in section 5.

2. EXPERIMENTAL ARRANGEMENT

The experimental arrangement consisting of a spherically bent mica crystal, a X-ray tube, and energy-resolving Si(Li)-detector, which were placed on the Rowland circle in the Johann configuration[4], is shown in Fig. 1. The mica crystal had a radius of curvature of 1524 mm and a reflecting surface size of 70 mm x 17 mm. The X-ray tube was a small air-cooled device with a copper anode. Both the spherically bent mica crystal and the X-ray tube were mounted within a common vacuum chamber, while the Si(Li)-detector was located outside the vacuum chamber behind a 20 μm thick polypropylene foil, which serve as a vacuum window. The foil was glued onto a blind flange with a borehole of 10 mm diameter. The Si(Li)-detector had a sensitive area with a diameter of 5 mm and was covered by a protective 8 μm thick beryllium foil. A copper plate with a 1 mm wide vertical slit was inserted between the detector and the polypropylene foil on the Rowland circle. In order to minimize the attenuation of low-energy X-rays in air, the inserted copper plate was in contact with the blind flange and the detector, so that the width of the air gap was less than 2 mm. The width of the slit of $w = 1$ mm defined the angular resolution $\Delta\theta$of the instrument. For measurements of the integrated reflectivity, w and $\Delta\theta$ were chosen to be larger than the Johann error[4] $(\Delta x)_J$ and the expected angular width $(\Delta\theta)_C$ from the intrinsic resolution and

mosaic spread of the crystal. The Johann error was $(\Delta x)_J$ = 0.28 mm for our experimental conditions. The value of $(\Delta\theta)_C$ was derived from the theoretical values of the spectral resolving power $(\lambda/\Delta\lambda)_C$ for mica crystals, which are listed in Table 1 of Ref. 2. For a Bragg angle of 50°, the listed theoretical values are $(\lambda/\Delta\lambda)_C$ = 1480 and $(\lambda/\Delta\lambda)_C$ = 4000 for reflection orders from 2 to 6 and reflection orders above 10, respectively. These values take into account a mosaic spread $\Delta\theta$ = 1 arcmin. The resolving power of $(\lambda/\Delta\lambda)_C$ = 1480 corresponds to an angular width of $(\Delta\theta)_C = 6.8 \times 10^{-4}$ or to a spatial resolution of $(\Delta x)_C$ = 0.73 mm at the position of the slit. The slit width of w = 1 mm was therefore larger than the expected combined error of $(\Delta x)_J$ and $(\Delta x)_C$.

We note that the position of the X-ray tube is not important for the present measurements. In principle, the X-ray tube could be located at any position inside or outside the Rowland circle. The Bragg angle and spectral resolution are both defined by the slit on the Rowland circle.

3. EXPERIMENTAL RESULTS

3.1 Measurements of the Bremsstrahlung Continuum

Figure 2 shows an overlay of two bremsstrahlung spectra from the X-ray tube. The measurements were made at two different times and under slightly different experimental conditions, meaning that the distance between the Si(Li)-detector and the polypropylene foil, which served as a vacuum window, was slightly different. However, in both cases, this distance was less than 2 mm. The spectrum shown by the *red dotted* line is from an earlier measurement and was used in reference 1 for evaluation of the integrated reflectivity at a

Bragg angle of Θ = 45°. The spectrum shown by the *black solid* line was obtained from a more recent measurement taken at the time when additional measurements of the integrated reflectivity for Θ = 43°, 47°, and 50° were made. For the purpose of the overlay, the spectrum from the second measurement has been multiplied by a factor of 2.9. For both measurements of the bremsstrahlung continuum, the X-ray tube was placed in the line of sight of the Si(Li)-detector. For the more recent measurement, the air gap between the detector and the polyethylene foil was exactly the same as for the measurements of the Bragg peaks at Θ = 43°, 47°, and 50° and corresponded to the experimental arrangement described in section 2. The spectra shown in Fig.2 consist of the Cu Kα and Cu Kβ lines at 8.040 and 8.905 keV, respectively, and a bremsstrahlung continuum which extends up to the operating voltage of 10 kV. The strong peak at 1.78 keV, which corresponds to the Si Kα and Si Kβ lines at 1.734 and 1.836 keV, respectively, is ascribed to fluorescent radiation in the Si(Li)-detector. This peak was therefore not present in the radiation incident on the crystal during the measurements of the Bragg peaks. We infer from Figure 2 that the spectra are in excellent agreement for energies in the range from 3.5 to 10 keV. *This result leads to the important conclusion that, within this energy range, the experimental results from reference 1 and the present measurements are not affected by variations in the experimental conditions.* At low energies the intensity is reduced due to attenuation by the polypropylene vacuum window, air gap, and beryllium foil on the detector. The intensity differences of the spectra for energies below 3.5 keV are ascribed to the fact that the detector was closer to the vacuum window for the more recent measurement. The spectrum from the second measurement also shows a small peak at 0.94 keV representing the copper L-lines.

3.2 Measurements of the integrated reflectivity

The integrated reflectivity was measured by the ratio of the intensity under a Bragg peak and the intensity of the incident bremsstrahlung continuum at the relevant energy. To facilitate a comparison between experiment and theory, the measured intensity ratio for one, arbitrarily chosen, Bragg peak was normalized to the theoretically predicted value for the integrated reflectivity. It is crucial for the evaluation of the Bragg peaks that the presence of spectral lines in the incident bremsstrahlung continuum and the presence of weak fluorescent lines, which are emitted from the constituent elements of the crystal and crystal holder, are taken into account. These effects must be investigated for each Bragg angle separately.

Figure 3 presents the experimental data, which were obtained for a Bragg angle of 43°. The bremsstrahlung spectrum from the X-ray tube is shown in Fig. 3a and the energy-resolved spectrum of the Bragg reflected radiation from the 2^{nd} up to the 20^{th} order is shown in Fig. 3b, and - on an expanded scale - in Fig. 3c. The *black* vertical lines and the *red* dotted vertical lines designate the calculated energies for the Bragg peaks and the positions of the spectral lines of Cu and Si, respectively. The *green* dotted lines designate small additional peaks, which are not present in the incident bremsstrahlung spectrum and whose positions are independent of the Bragg angle. These peaks are due to fluorescent radiation from the crystal and crystal holder and correspond to the Kα and Kβ lines of Al, S, K, Mn, Cr, and Fe. The strongest lines are the Kα and Kβ lines of Al and K at 1.5 keV and 3.3 keV. A significant contribution to the Al Kα line originates from the crystal holder, which was fabricated out of aluminum. Also Cr and Fe are major constituents of mica crystals. The fluorescent peaks from S, Mn, Cr and Fe are much weaker than those of Al and K. These fluorescent peaks can

interfere with the measurements of the integrated reflectivity if they coincide with the position of Bragg peaks and if the Bragg peaks are small. Whether such interferences exist must be carefully checked for each Bragg angle. Fig. 3c also shows the presence of some detector noise at the lowest energies. This detector noise affects the evaluation of the integrated reflectivity for the second and, to a lesser extent, fourth order of reflection.[5]

The observed width and shape of the Bragg peaks are determined by the energy resolution of the Si(Li)-detector of 155 eV FWHM. However, the range of energies, which contribute to each Bragg peak, is much narrower and of the order of a few eV, since the resolution of the crystal spectrometer is $\lambda/\Delta\lambda = 1500 - 4000$, depending on the Bragg angle. We may therefore conclude that, for $\Theta = 43°$, the observed Bragg peaks are well separated from any spectral lines - except for the Bragg peak of the 18^{th} order, which is very close to the Cu Kα line. The Cu Kα line may therefore interfere with the measurement of the integrated reflectivity for the 18^{th} order.

The intensity under each Bragg peak was determined from a least squares fit of a Gaussian with a FWHM of 155 eV as shown in Fig. 4. An important point of the data analysis - which was overlooked in reference 1 and which was the cause for the 'apparent' discrepancies between the experiment and theory - is that the width of the energy interval ΔE that contributes to a Bragg reflection varies with the energy E of the Bragg peak according to the equation, $\Delta\lambda/\lambda = \Delta E/E = \Delta\Theta/\tan(\Theta) = \text{constant}$, since the measurements were performed at a constant Bragg angle Θ and a constant $\Delta\Theta$.For an evaluation of the integrated reflectivity, the intensity under a Bragg peak must be divided by the intensity, $I(E)\cdot\Delta E$, of the incident bremsstrahlung, where I(E) is the bremsstrahlung intensity at the energy E, and ΔE is

proportional to E. The error in the data analysis of reference 1 was that ΔE was kept constant for all the Bragg peaks independent of their energies.

Another important point for the data analysis is that, in the vicinity of a spectral line, one must take the interpolated intensity of the bremsstrahlung spectrum (see Fig. 3 a), rather than the intensity including the spectral line, if the separation between the center positions of the Bragg peak and the spectral line is larger than ≈ 5 eV, since the observed broad 'apparent' line profiles are only an artifact due to the finite resolution of the Si(Li)-detector.

Following these procedures, we have obtained the experimental values for the integrated reflectivity, which are shown in Fig. 5 together with the theoretical predictions from reference 2. These theoretical predictions include the value from the dynamic theory[6,7] and the kinematic limit. The experimental results have been normalized by setting the experimental value for the 8th order of reflection equal to the corresponding dynamic value of 4.4762 μrad from the theory[2]. The experimental values are shown by the *black* solid lines, and the theoretical values from the dynamic theory and the kinematic limit are shown by the *red* and *blue* lines, respectively. We infer from Fig. 5 that – except for the 12th and 18th order of reflection – the experimental values are between (or close to) the theoretically predicted values of the dynamic theory and kinematic limit.

The observed deviation for the 18th order of reflection may be due to an interference with the Cu Kα line. The experimental values for the integrated reflectivity of the 2nd and 4th order of reflection are less certain, since the evaluation of these Bragg peaks is affected by the elevated background at low energies due to detector noise and by a small fluorescent peak at 2.3 keV, which may be ascribed to the L-lines of high-Z elements, such as Mo, and since the (measured) intensity of the incident bremsstrahlung spectrum at the position of the 2nd

order peak is very small. However, the experimental uncertainties are smaller for the 4^{th} order than for the 2^{nd} order. The experimental values for the 6^{th} up to the 20^{th} order, which fall into the energy range from 3 to 10 keV, should be very reliable - with exception of the 18^{th} order, which may be impaired by the vicinity of the Cu Kα line.

The same general comments apply to Figures 6 – 11, which represent the results for the Bragg angles 47° and 50°. There are a few additional observations. The fluorescent peak at 3.3 keV from potassium (K) interferes with the 8^{th} order Bragg peak for the Bragg angles of 47° and 50°, requiring a small correction for the measured integrated reflectivity for the 8^{th} order. Moreover, for the Bragg angle of 50°, there is an interference between the Bragg peak of the 22^{nd} order and the Cu Kα line. Dividing by the extrapolated bremsstrahlung spectrum is here not justified, since the 22^{nd} order Bragg peak is too close to the Cu Kα line and since it is difficult to determine the exact contribution from the Cu Kα line. The experimental value for the integrated reflectivity of the 22^{nd} order is therefore not reliable.

Also shown in Fig. 12 are the corrected experimental values for the integrated reflectivity for the Bragg angle of 45°. The raw data for the bremsstrahlung spectrum and Bragg peaks were already shown in Figs. 2 and 3 of reference 1.

We note that the experimental values for the integrated reflectivity of the 12^{th} and 18^{th} order are higher than the kinematic limit for all the investigated Bragg angles. Since - for the Bragg angles of 47° and 50° - the 18^{th} order Bragg peak is well separated from the Cu Kα line, an interference of the Cu Kα line with the 18^{th} order Bragg peak can be excluded for these Bragg angles. We are therefore led to conclude that there is still a systematic difference between the experimental results and the theoretical predictions for the 12^{th} and 18^{th} order of reflection.

4. Advantages of the new method.

The new method of measuring integrated reflectivity described in this paper offers many advantages over the previously used technique, which is illustrated in Fig. 7 of reference 2. The previous technique employs monochromatic radiation of characteristic X-ray lines, such as the Cu Kα line at 0.154056 nm and the Mo Kα line at 0.07093 nm, from the anode of an X-ray tube. This line radiation is separated from the bremstrahlung continuum by Bragg reflection from a monochromator crystal and then directed onto the sample crystal. The cross-section of the incident monochromatic beam and the corresponding X-ray spot on the sample crystal is about 1 mm^2. The sample crystal is rotated through a small range of Bragg angles around the Bragg angle for which the maximum reflectivity is expected, and the reflected X-ray intensity is monitored with an X-ray detector, e. g. a scintillator or a photomultiplier tube, which is only used only as a photon counter.

The previouly used technique is very tedious and time consuming and it can be readily used only for a limited number of X-ray energies, those corresponding to the Kα lines of available anodes. In fact, a change of the energy requires the installation of a different anode in the X-ray tube. Moreover, the measurement of each Bragg reflection requires a new alignment of the sample crystal and detector and subsequent scanning of the sample crystal through a range of Bragg angles. We also point out that this technique provides the integrated reflectivity for the different orders of reflection for a *predetermined energy*, namely, the energy of the characteristic X-ray lines from the anode, and <u>not</u> for a *predetermined Bragg angle*, which is of more immediate interest for the calibration of a crystal spectrometer.

In contrast to the previously used technique, the new method can provide the integrated reflectivity for *any* X-ray energy since the incident radiation consists of the bremsstrahlung continuum, instead of the characteristic line radiation. The new method is therefore independent of the material of the anode and can be used with any X-ray tube. The upper limit of the energy range of the bremsstrahlung continuum can be simply adjusted by changing the high voltage applied to the X-ray tube.

Since the new method yields the integrated reflectivity for different orders of reflection simultaneously at a predetermined Bragg angle with one fixed experimental arrangement, it is very well suited for an *in situ* calibration of a crystal spectrometer, which is usually set up for a certain Bragg angle. The obtained relative values of the integrated reflectivity for the different orders of reflection are very accurate and are not affected by fluctuations in the X-ray intensity from the X-ray tube, since all the Bragg peaks are measured simultaneously. It is therefore not necessary to monitor the X-ray flux from the X-ray tube. Moreover, the integrated reflectivity is measured for a narrow energy interval of a few eV that corresponds to the spectral resolution of the spectrometer, while with the previously used technique the energy interval is typically about 20-40 eV wide, since it includes both the characteristic $K\alpha$- and $K\beta$ lines from the anode.

Further advantages of the new method are due to the fact that the entire crystal is illuminated by the X-ray tube. The throughput, which is proportional to the illuminated area of the crystal, can therefore be orders of magnitude larger than that of the previously used technique, where the area of the X-ray spot on the crystal is typically only about 1 mm^2. The new method also yields the integrated reflectivity of the entire crystal, whereas the previously used techniques yields the integrated reflectivity from only a small, about 1 mm^2, area of the

crystal. To measure the integrated reflectivity of the different orders of reflection from the entire crystal with the previously used technique would be very tedious (or practically impossible), since it requires scanning of the incident monochromatic X-ray beam over the crystal surface. This process would have to be repeated for the Bragg reflections of each order.

Another advantage is due to the fact that the new method uses the X-ray flux directly from an x-ray tube, rather than X-rays of greatly reduced intensity diffracted from a pre-selector crystal, as is the case with the previously used technique. Therefore, much lower power can be used on the x-ray tube. This fact has two favorable implications: (1) much cheaper and smaller air-cooled x-ray tubes can be used, rather than expensive, heavy, bulky water-cooled tubes, which might be needed for the previously used technique; and (2) radiation shielding and personnel radiation protection requirements are greatly reduced. This lower flux requirement allows, for instance, the use of *'home-made',* low-power, and windowless, X-ray tubes, which can be directly connected to the vacuum of the spectrometer chamber. Such X-ray tubes are of particular interest for the investigation of low-energy X-rays below 1 keV. We point out that commercially available high-power X-ray tubes are usually manufactured with vacuum windows, which severely attenuate the X-ray intensity at energies below 1 keV. We also point out that the accessible energy range can be extended from 0.2 to 100 keV with the use of windowless Si (Li)- detectors for low X-ray energies and Ge-diode detectors for high X-ray energies.

With the new method it is also possible to observe, in addition to the Bragg peaks, the fluorescent radiation from the constituents of the material under investigation. This

possibility will be of interest for an *in situ* analysis of structures, such as multi-layer structures, during the manufacturing process.

5. CONCLUSIONS

In an effort to verify our earlier results from reference 1, additional measurements of the integrated reflectivity have been performed at Bragg angles of 43°, 47° and 50°. Special care was taken to assure the uniformity of the experimental conditions for measurements of the Bragg peaks and the incident bremsstrahlung continuum. Moreover, corrections for contributions from fluorescent peaks were made, where necessary. In the course of these investigations, we discovered that the apparent discrepancies between theory and experiment - that had been found in reference 1 - were actually due to an oversight in the data analysis. After correcting for this oversight we now obtain very good agreement between theory and experiment for the entire spectral range. A detailed description of the experimental results and data analysis has been given in this paper for future reference.

ACKNOWLEDGEMENTS

We would like to thank Dr. A. Ya. Faenov and Dr. A. England for valuable discussions. M. Bitter gratefully acknowledges the hospitality and support of Dr. G. S. Lee and Dr. M. Kwon during his stay at the Korea Basic Science Institute. This work was supported by the Korean Ministry of Science and Technology, the Korean Federation of Science and Technology Societies, and the US-Korea collaboration under the US Department of Energy Contract No. DE-AC02-76-CHO-3073.

REFERENCES

1. S. G. Lee, J. G. Bak, Y. S. Jung, M. Bitter, K. W. Hill, O. Wehrhan, E. Foerster, Proceedings of SPIE **4501**, 177 (2001).
2. G. Hölzer, O. Wehrhan, J. Heinish, E. Förster, T. A. Pikuz, Ya Faenov, S. A. Pikuz, V. M. Romanova and T. A. Shelovenko, Physica Scripta **57**, 301 (1998).
3. G. Hoelzer, O. Wehrhan, E. Foerster: Cryst. Res. Technol. **33**, 555 (1988).
4. H. H. Johann, Z. Phys. **69**, 185 (1931).
5. Here, we adopt the characterization of mica crystals from Ref. 2, assuming a lattice constant of d = 19.9149 Å (private communication by Dr. A. Ya. Faenov), where even orders of reflection are allowed and odd orders of reflection are forbidden due to crystal symmetry. In the literature, the value of 19.9149 Å is often given as the value of the 2d-spacing and no distinction is made between odd and even orders of reflection, i.e., all orders of reflection are allowed.
6. D. Taupin, Buill. Soc. Franc. Miner. Crist. **87**, 469 (1964).
7. Z. G. Pinsker, "Dynamical scattering of X-rays in crystals", Springer-Verlag, Berlin/Heidelberg/New York (1979).

FIGURE CAPTIONS

Figure 1: Experimental arrangement.

Figure 2: Overlay of two emission spectra from the X-ray tube. The spectra were obtained for slightly different experimental conditions and are explained in the text

Figure 3: Raw spectral data**.** The subfigures 3a shows the emission spectrum from the X-ray tube, and subfigures 3b and 3c show the Bragg reflected radiation from the mica crystal for $\Theta = 43°$ on different scales.

Figure 4: Observed Bragg peaks *(in red)* for $\Theta = 43°$ and least squares fits of Gaussians *(black solid lines)* with a FWHM of 155 eV corresponding to the energy resolution of the Si(Li) detector.

Figure 5: Comparison of the experimental and predicted values for the integrated reflectivity for $\Theta = 43°$. To facilitate the comparison, the experimental values have been normalized by setting experimental value for the 8^{th} order of reflection equal to the value predicted by the dynamical theory. The experimental values are shown by the *black solid lines*, and the theoretical values from the dynamic theory and the predicted kinematic limit are shown by the *red* and *blue* lines.

Figure 6: Raw spectral data for $\Theta = 47°$**.**

Figure 7: Observed Bragg peaks *(in red)* for $\Theta = 47°$ and least squares fits of Gaussians *(black solid lines).*

Figure 8: Comparison of the experimental and predicted values for the integrated reflectivity for $\Theta = 47°$.

Figure 9: Raw spectral data for $\Theta = 50°$**.**

Figure 10: Observed Bragg peaks *(in red)* for $\Theta = 50°$ and least squares fits of Gaussians *(black solid lines).*

Figure 11: Comparison of the experimental and predicted values for the integrated reflectivity for $\Theta = 50°$.

Figure 12: Comparison of the experimental and predicted values for the integrated reflectivity for $\Theta = 45°$.

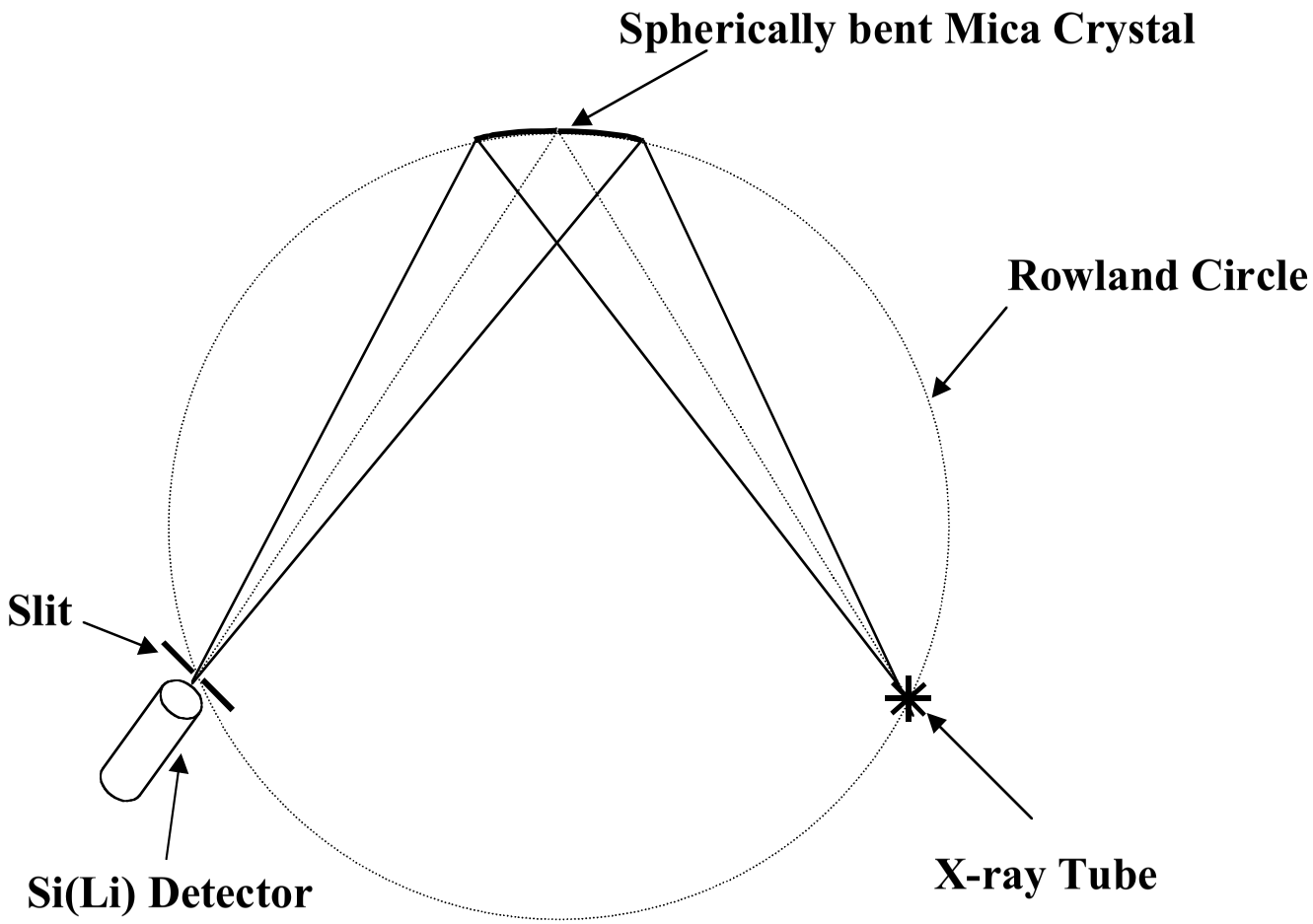
Spherically bent Mica Crystal
Rowland Circle
Slit
Si(Li) Detector
X-ray Tube

Figure 1

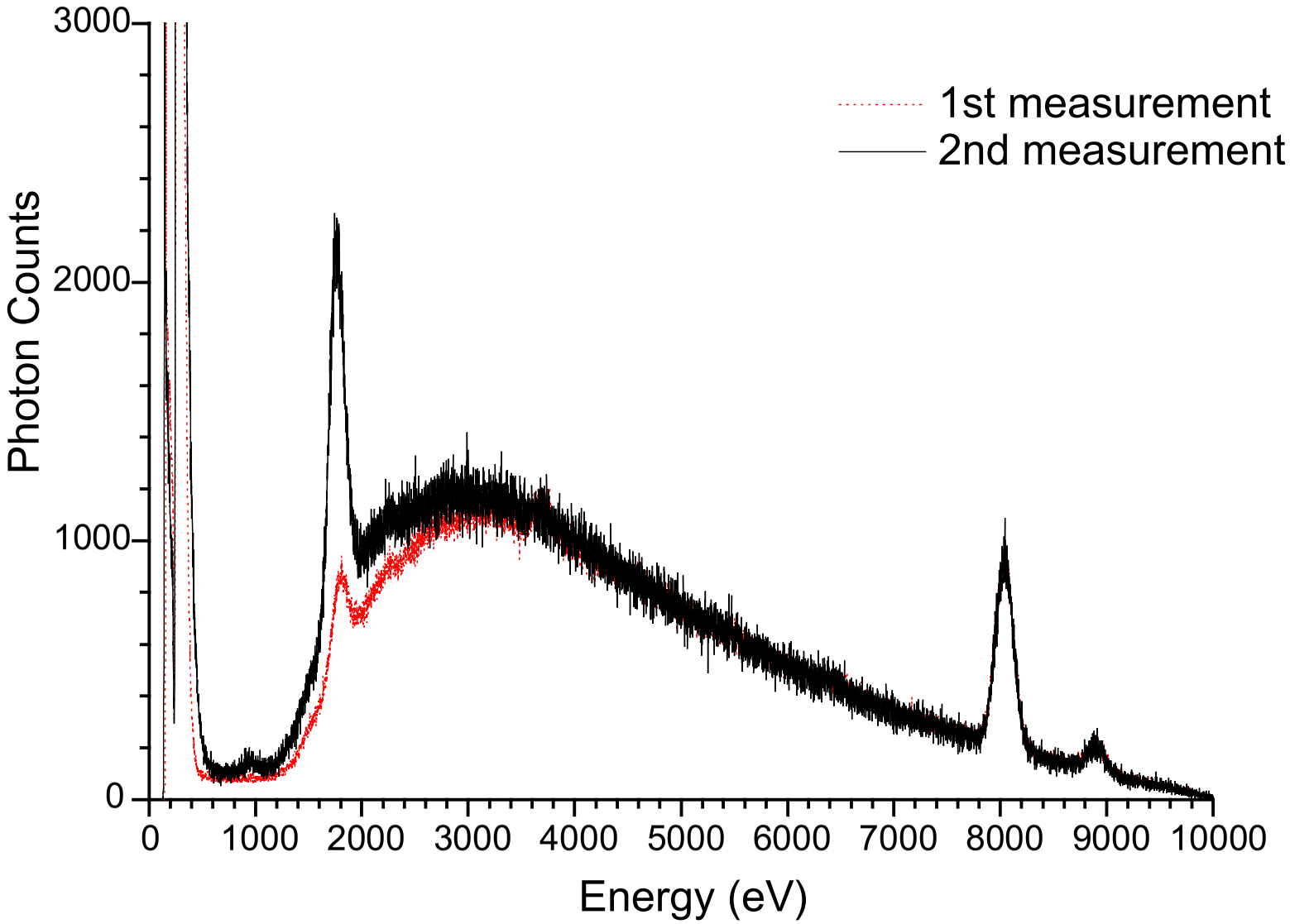
Photon Counts
Energy (eV)
1st measurement
2nd measurement
0
1000
2000
3000
4000
5000
6000
7000
8000
9000
10000

Figure 2

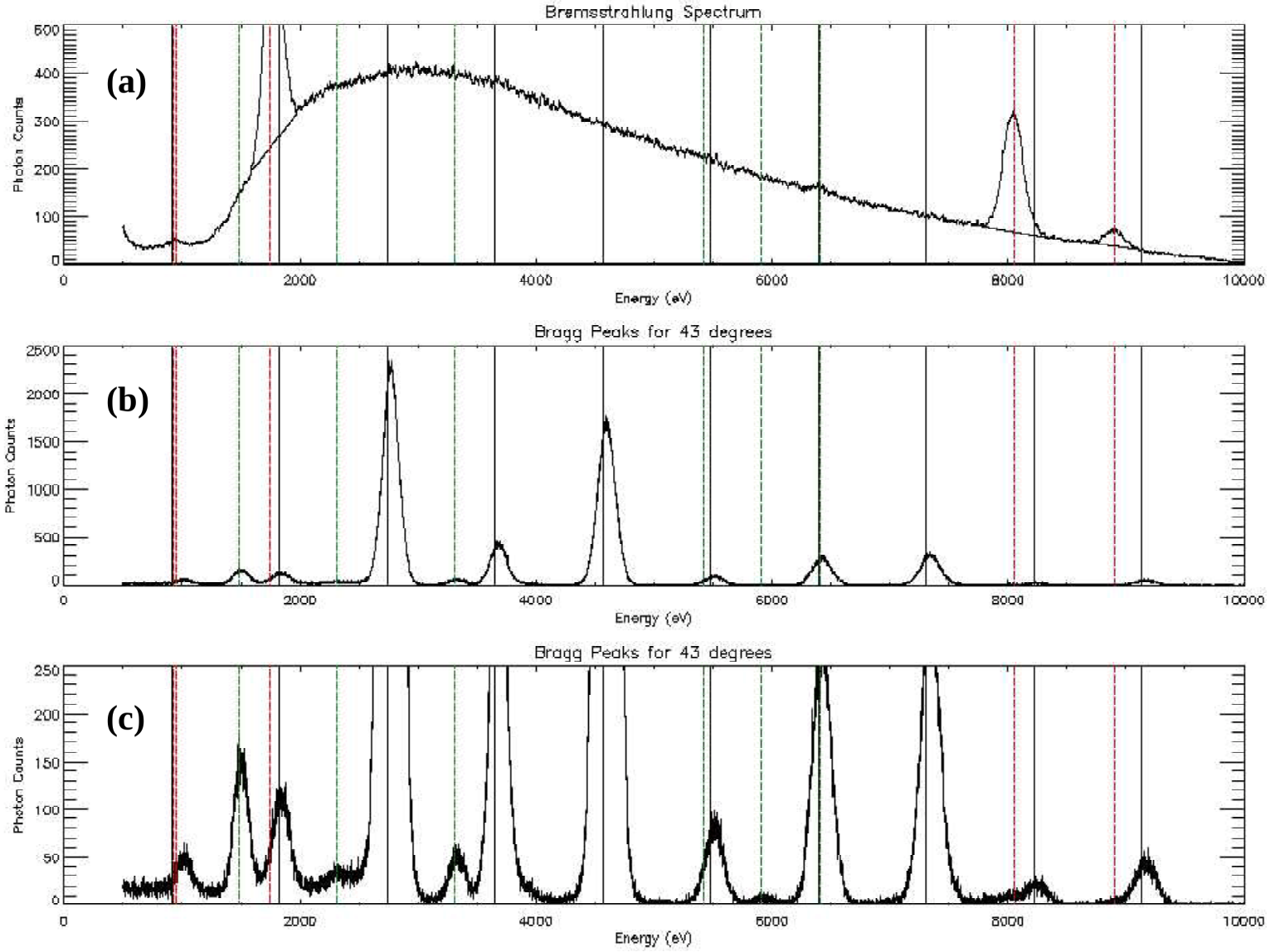
Bremsstrahlung Spectrum
(a)
Photon Counts
Energy (eV)
Bragg Peaks for 43 degrees
(b)
Photon Counts
Energy (eV)
Bragg Peaks for 43 degrees
(c)
Photon Counts
Energy (eV)

Figure 3

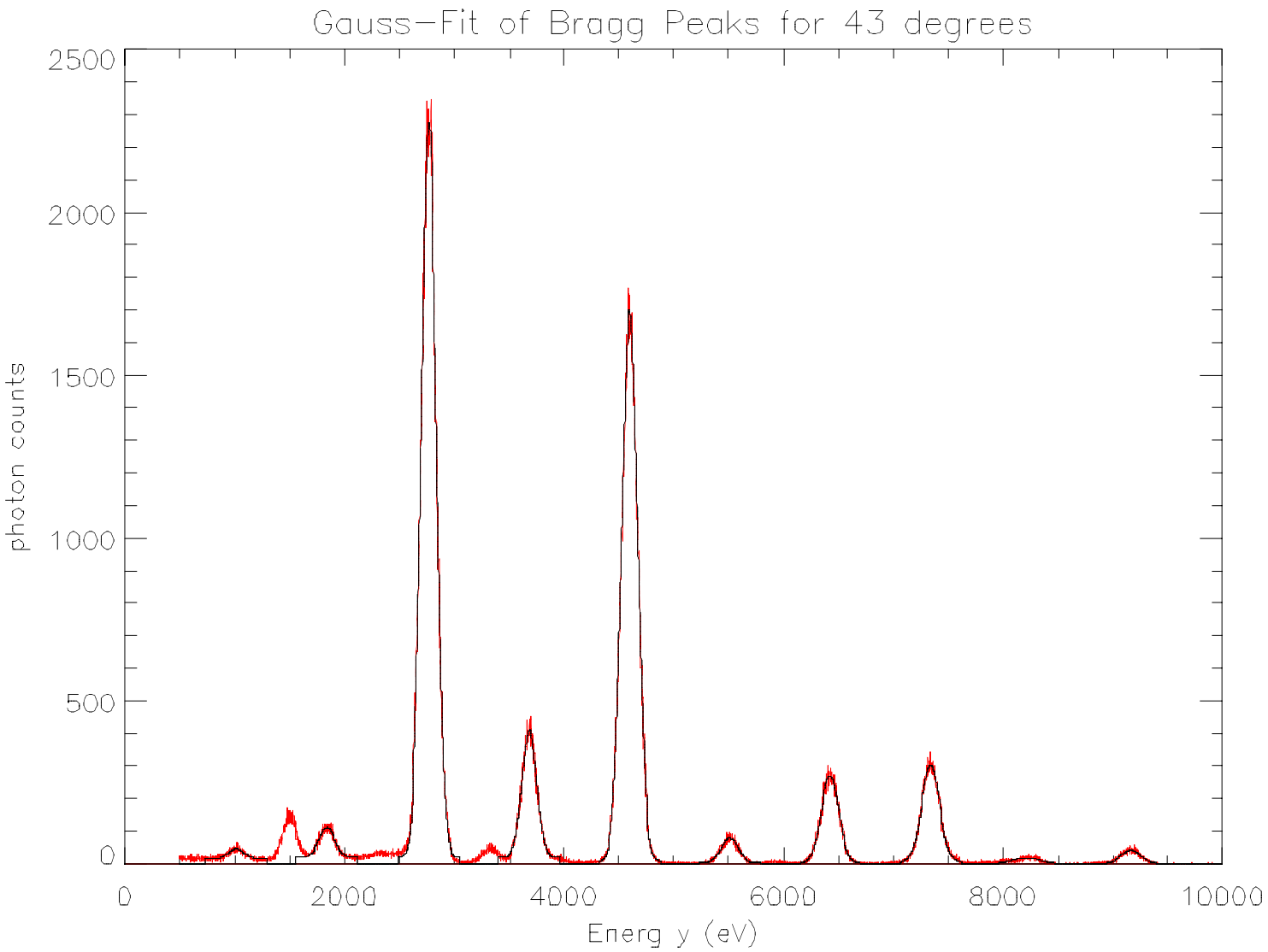
Gauss-Fit of Bragg Peaks for 43 degrees
photon counts
2500
2000
1500
1000
500
0
0
2000
4000
6000
8000
10000
Energy (eV)

Figure 4

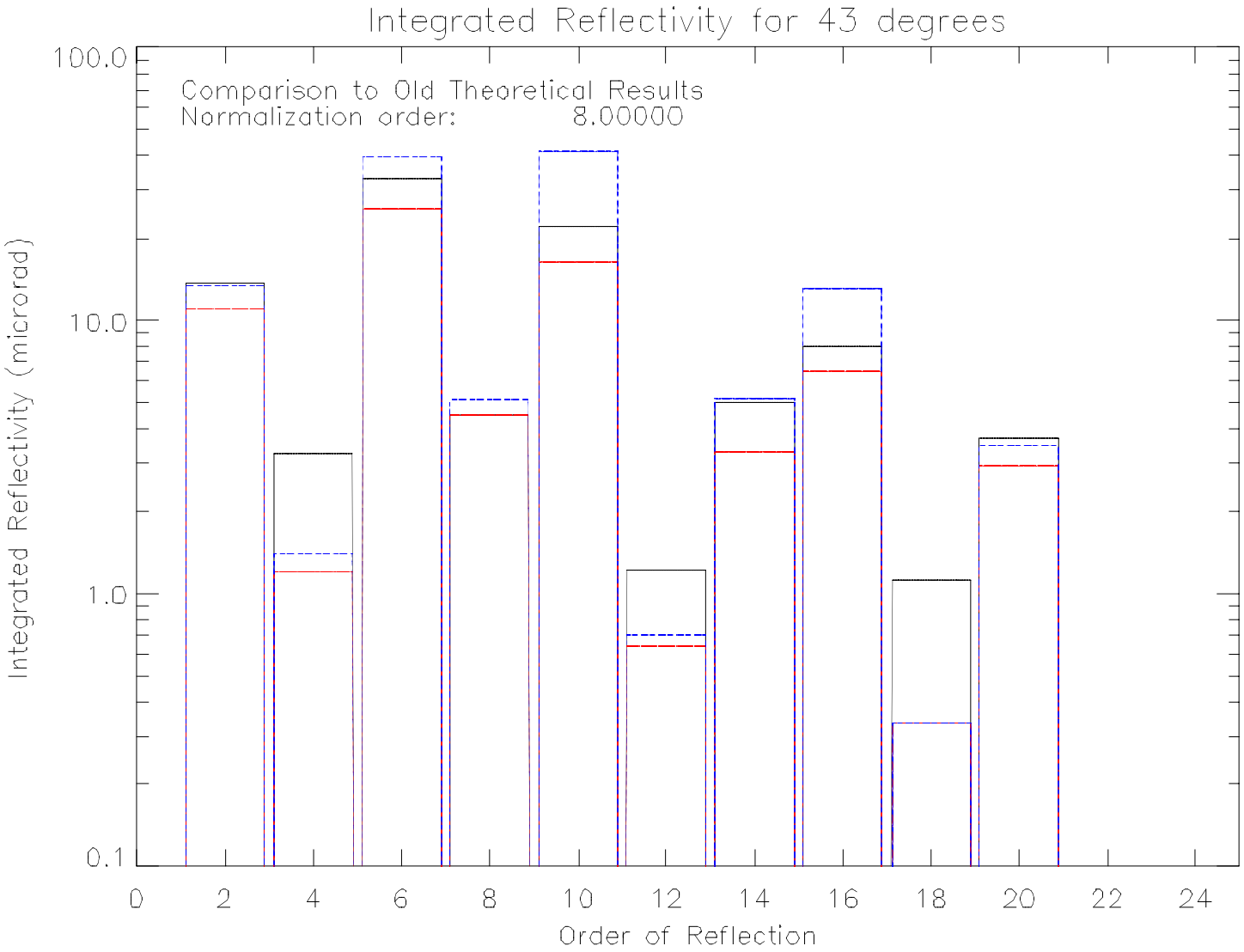
Integrated Reflectivity for 43 degrees
Comparison to Old Theoretical Results
Normalization order: 8.00000
Integrated Reflectivity (microrad)
100.0
10.0
1.0
0.1
0
2
4
6
8
10
12
14
16
18
20
22
24
Order of Reflection

Figure 5

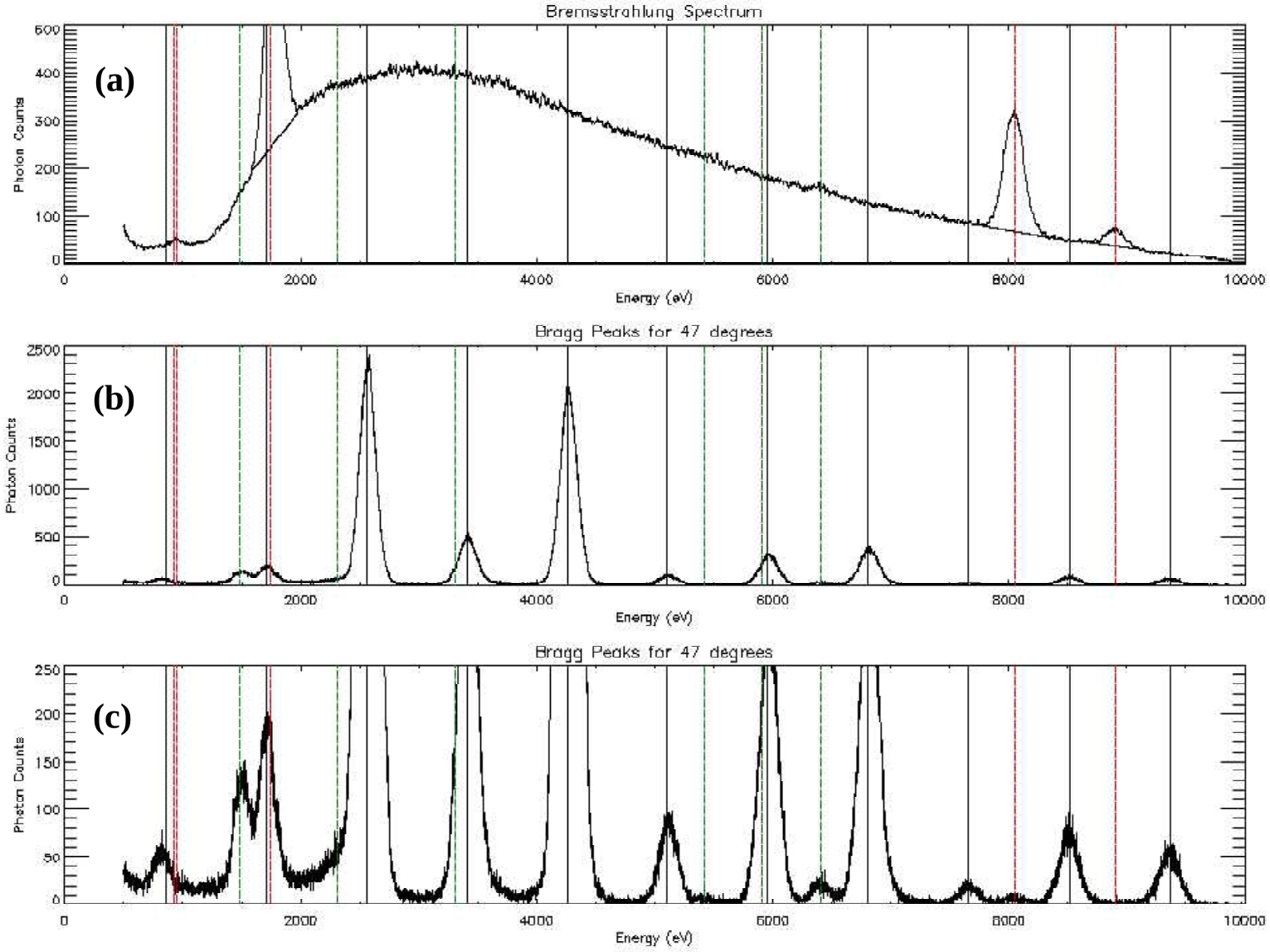
Bremsstrahlung Spectrum
(a)
Photon Counts
Energy (eV)
Bragg Peaks for 47 degrees
(b)
Photon Counts
Energy (eV)
Bragg Peaks for 47 degrees
(c)
Photon Counts
Energy (eV)

Figure 6

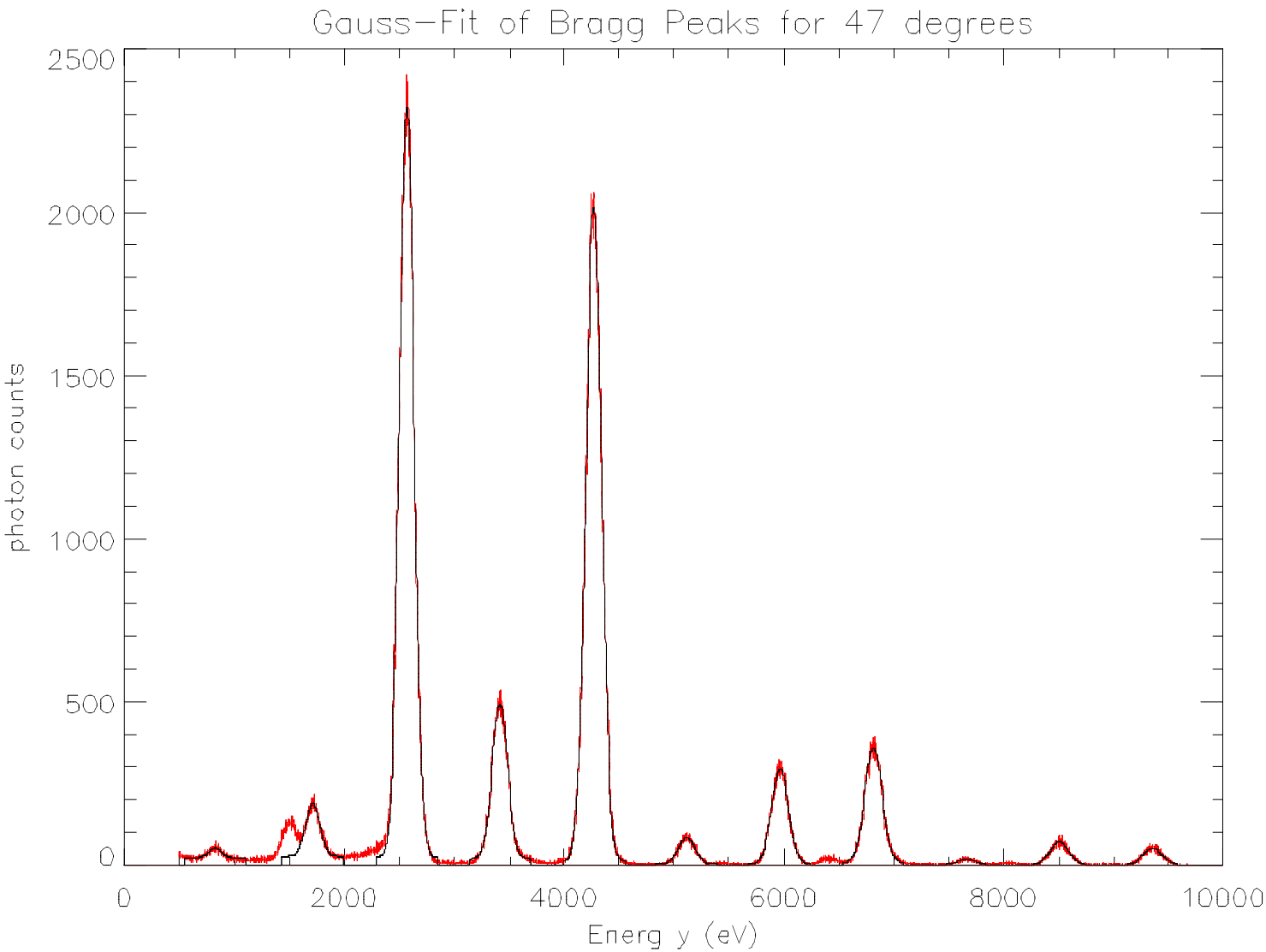
Gauss−Fit of Bragg Peaks for 47 degrees
photon counts
2500
2000
1500
1000
500
0
0
2000
4000
6000
8000
10000
Energ y (eV)

Figure 7

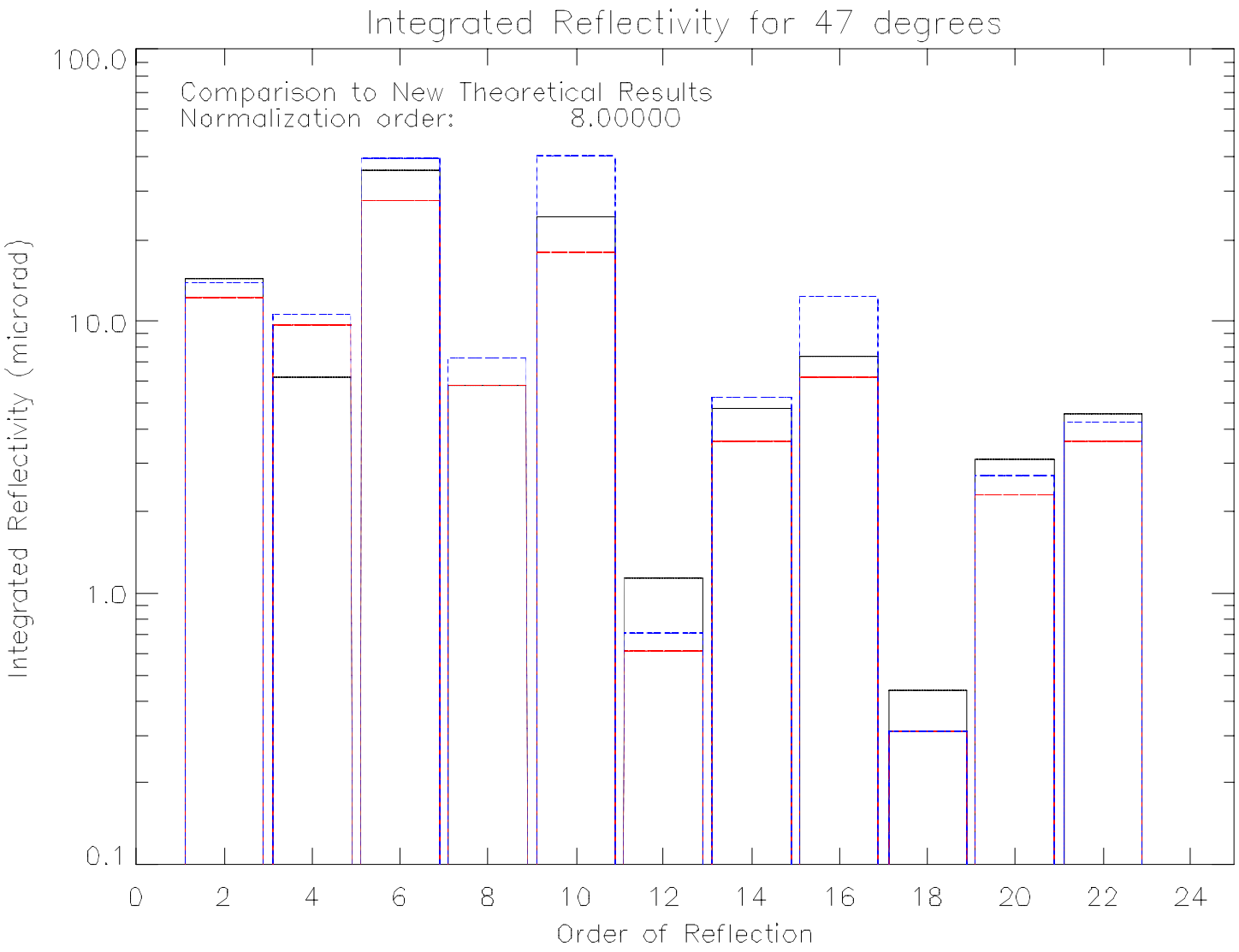
Integrated Reflectivity for 47 degrees
Comparison to New Theoretical Results
Normalization order: 8.00000
Integrated Reflectivity (microrad)
100.0
10.0
1.0
0.1
0
2
4
6
8
10
12
14
16
18
20
22
24
Order of Reflection

Figure 8

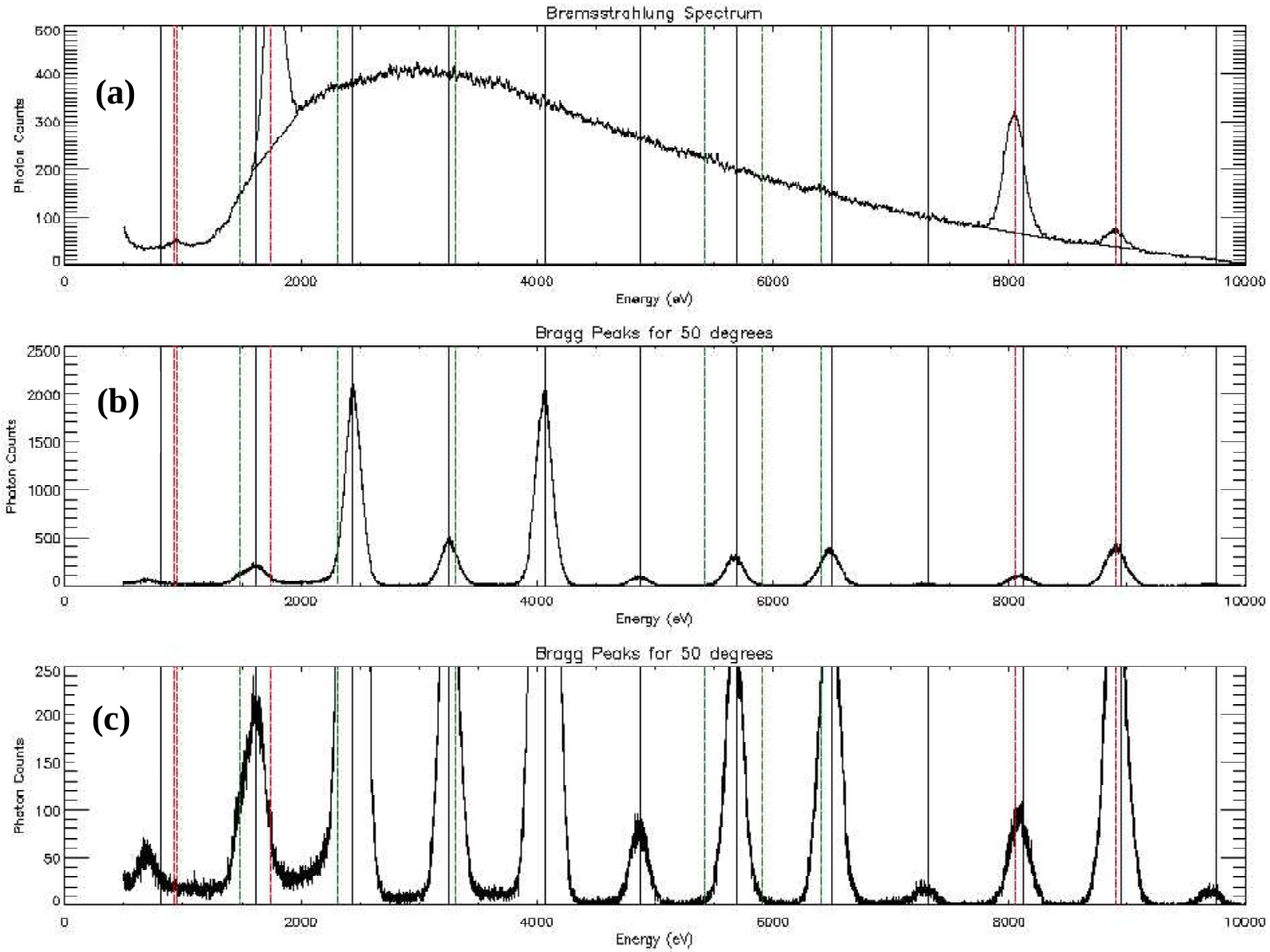
Bremsstrahlung Spectrum
(a)
Photon Counts
Energy (eV)
Bragg Peaks for 50 degrees
(b)
Photon Counts
Energy (eV)
Bragg Peaks for 50 degrees
(c)
Photon Counts
Energy (eV)

Figure 9

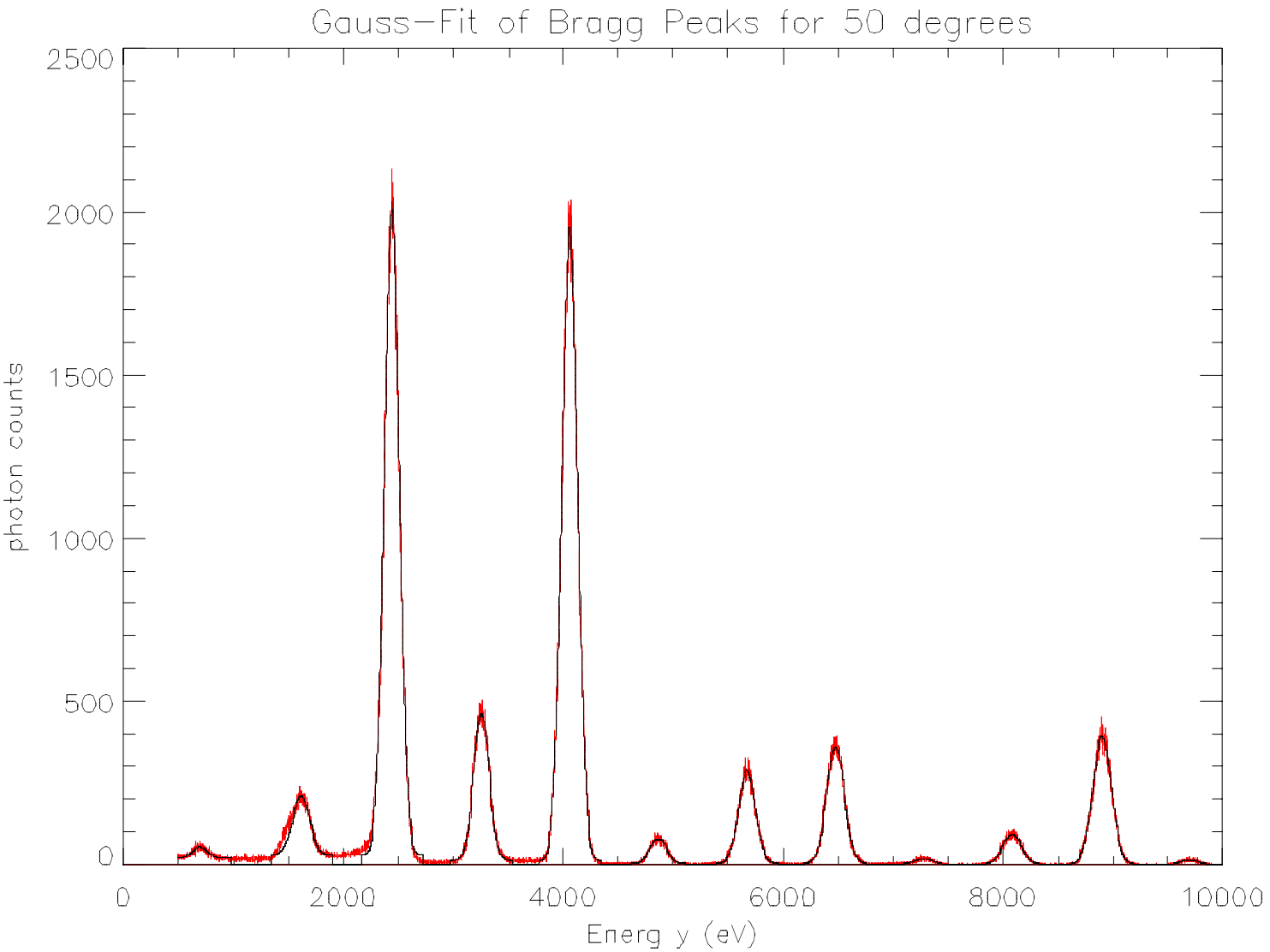
Gauss−Fit of Bragg Peaks for 50 degrees
photon counts
2500
2000
1500
1000
500
0
0
2000
4000
6000
8000
10000
Energ y (eV)

Figure 10

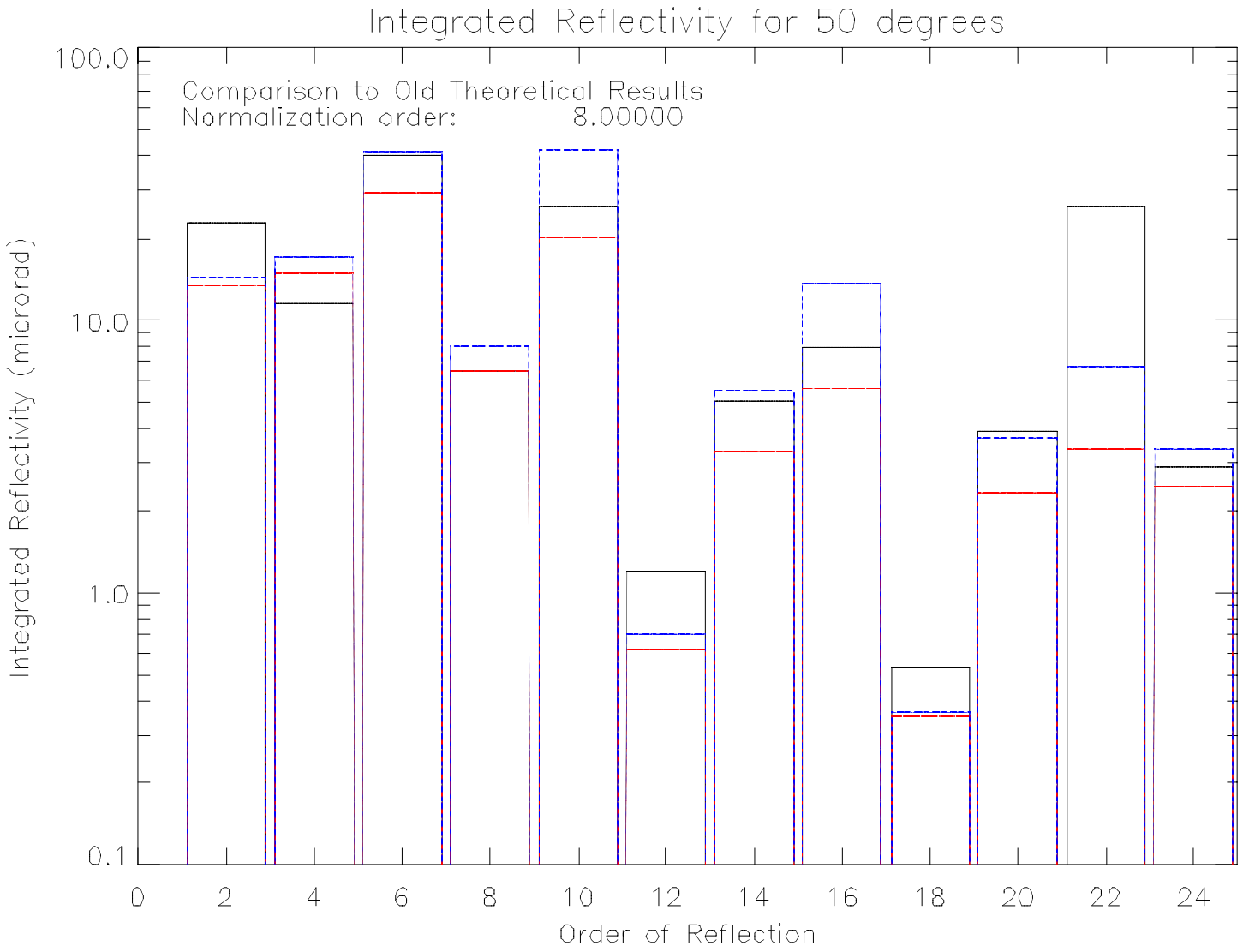
Integrated Reflectivity for 50 degrees
Comparison to Old Theoretical Results
Normalization order: 8.00000
Integrated Reflectivity (microrad)
100.0
10.0
1.0
0.1
0
2
4
6
8
10
12
14
16
18
20
22
24
Order of Reflection

Figure 11

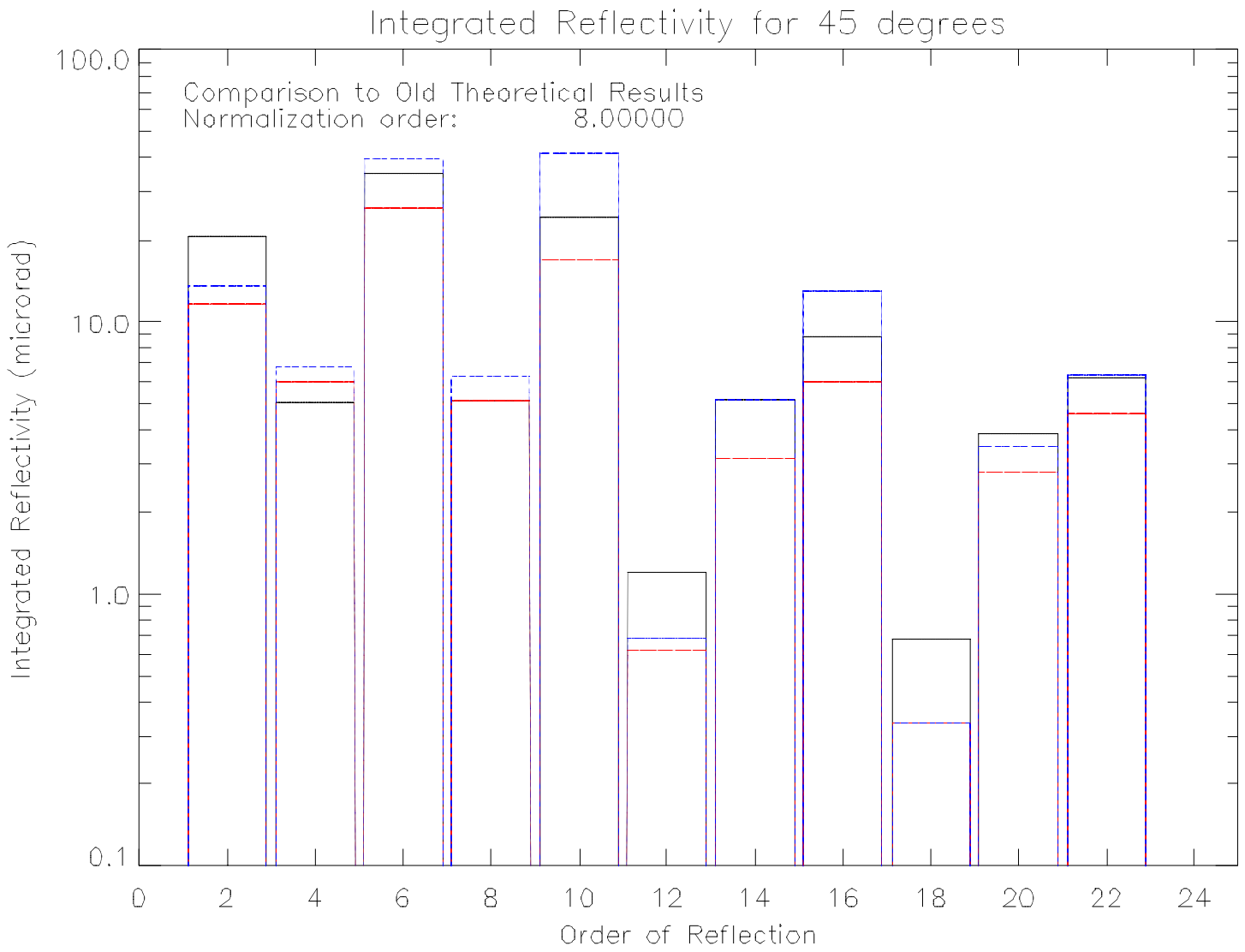
Integrated Reflectivity for 45 degrees
Comparison to Old Theoretical Results
Normalization order: 8.00000
100.0
10.0
1.0
0.1
Integrated Reflectivity (microrad)
0
2
4
6
8
10
12
14
16
18
20
22
24
Order of Reflection

Figure 12

External Distribution

Plasma Research Laboratory, Australian National University, Australia
Professor I.R. Jones, Flinders University, Australia
Professor João Canalle, Instituto de Fisica DEQ/IF - UERJ, Brazil
Mr. Gerson O. Ludwig, Instituto Nacional de Pesquisas, Brazil
Dr. P.H. Sakanaka, Instituto Fisica, Brazil
The Librarian, Culham Laboratory, England
Mrs. S.A. Hutchinson, JET Library, England
Professor M.N. Bussac, Ecole Polytechnique, France
Librarian, Max-Planck-Institut für Plasmaphysik, Germany
Jolan Moldvai, Reports Library, MTA KFKI-ATKI, Hungary
Dr. P. Kaw, Institute for Plasma Research, India
Ms. P.J. Pathak, Librarian, Insitute for Plasma Research, India
Ms. Clelia De Palo, Associazione EURATOM-ENEA, Italy
Dr. G. Grosso, Instituto di Fisica del Plasma, Italy
Librarian, Naka Fusion Research Establishment, JAERI, Japan
Library, Plasma Physics Laboratory, Kyoto University, Japan
Research Information Center, National Institute for Fusion Science, Japan
Dr. O. Mitarai, Kyushu Tokai University, Japan
Dr. Jiangang Li, Institute of Plasma Physics, Chinese Academy of Sciences, People's Republic of China
Professor Yuping Huo, School of Physical Science and Technology, People's Republic of China
Library, Academia Sinica, Institute of Plasma Physics, People's Republic of China
Librarian, Institute of Physics, Chinese Academy of Sciences, People's Republic of China
Dr. S. Mirnov, TRINITI, Troitsk, Russian Federation, Russia
Dr. V.S. Strelkov, Kurchatov Institute, Russian Federation, Russia
Professor Peter Lukac, Katedra Fyziky Plazmy MFF UK, Mlynska dolina F-2, Komenskeho Univerzita, SK-842 15 Bratislava, Slovakia
Dr. G.S. Lee, Korea Basic Science Institute, South Korea
Institute for Plasma Research, University of Maryland, USA
Librarian, Fusion Energy Division, Oak Ridge National Laboratory, USA
Librarian, Institute of Fusion Studies, University of Texas, USA
Librarian, Magnetic Fusion Program, Lawrence Livermore National Laboratory, USA
Library, General Atomics, USA
Plasma Physics Group, Fusion Energy Research Program, University of California at San Diego, USA
Plasma Physics Library, Columbia University, USA
Alkesh Punjabi, Center for Fusion Research and Training, Hampton University, USA
Dr. W.M. Stacey, Fusion Research Center, Georgia Institute of Technology, USA
Dr. John Willis, U.S. Department of Energy, Office of Fusion Energy Sciences, USA
Mr. Paul H. Wright, Indianapolis, Indiana, USA

The Princeton Plasma Physics Laboratory is operated
by Princeton University under contract
with the U.S. Department of Energy.

Information Services
Princeton Plasma Physics Laboratory
P.O. Box 451
Princeton, NJ 08543

Phone: 609-243-2750
Fax: 609-243-2751
e-mail: pppl_info@pppl.gov
Internet Address: http://www.pppl.gov